Environmental baselines and reconstruction of Atlantic Water inflow in Bjørnøyrenna, SW Barents Sea, since 1800 CE

Noortje Dijkstra[1*], Juho Junttila[1], and Steffen Aagaard-Sørensen[1]

[1]Department of Geosciences, UiT The Arctic University of Norway in Tromsø, Postboks 6050 Langnes, N-9037 Tromsø, Norway

* Corresponding author: noortje.dijkstra@uit.no Telephone: +47 776 23313

Highlights

- Natural variability and Atlantic water inflow into the Barents Sea was investigated
- Metal concentrations correspond to no effect levels
- Foraminifera show presence of Atlantic water around termination of Little Ice age
- Atlantic water inflow was reduced between 1900 and 1980 CE
- Benthic foraminiferal assemblages show enhanced Atlantic water inflow after 1980 CE

Abstract

Metal concentrations, sediment properties and benthic foraminiferal assemblages were investigated in sediment cores in the SW Barents Sea, to reconstruct environmental baselines and natural variability of Atlantic Water inflow since 1800 CE. Metal concentrations correspond to no effect levels and do not influence the foraminifera. Increased Hg and Pb was linked to inflow of Atlantic Water. The data set is considered to reflect the pre-impacted environmental baseline and range in natural variability of the study area. The foraminiferal assemblages in the SW part of the study area showed warming and presence of Atlantic Water towards 1900 CE. The NE part of the region indicate presence of cold Artic Water influenced conditions. Between 1900 and 1980 CE, the SW region indicates reduced inflow of Atlantic Water. From 1980 CE towards the present the assemblages of the entire study area show warming of Atlantic Water and northward retreat of the Arctic Front.

Keywords: benthic foraminifera, heavy metals, natural variability, sediments, Atlantic Water, Arctic Water, Anthropocene, Barents Sea, biomonitoring, cores

1. Introduction

The Barents Sea is a unique and highly sensitive shallow water polar ecosystem, highly susceptible to changes in converging ocean currents (Sakshaug, 1997). The Barents Sea is one of the world's most productive seas, in particular around the oscillating ice edge (Sakshaug, 1997). In recent decades, the Barents Sea has experienced a fast growth in human activities, which is expected to continue and further diversify in the coming years. Of particular concern are activities related to the petroleum industry, including release of drill cuttings to the seafloor. Drill cuttings are by-products of both oil- and gas drilling and contain fine-grained slurry of rock and heavy metals. It is of importance that such deposits are accurately monitored and managed. One way of monitoring environmental impact is by assessing changes in the seafloor fauna (bio-monitoring) (WFD, 2000). Following the EU legislation, the impact of enhanced environmental pressure is assessed by the extent of deviation of the benthic community from reference conditions (WFD, 2000). Reference conditions correspond to *"biological, chemical and morphological conditions associated with no or very low human pressure"* (WFD, 2000). It is therefore of great relevance to not only understand the local impact of petroleum activity, but also to establish reliable reference conditions reflecting the pre-impacted environmental baseline, especially in areas not yet opened for petroleum production. This will serve as future reference to monitor the environmental impact of anthropogenic activity. Although monitoring changes in these reference conditions can indicate the environmental impact of increased anthropogenic activity in the Barents Sea, effects of natural environmental changes will be superimposed on these anthropogenic induced changes. The applicability of an environmental baseline must therefore always take the natural variability of the processes and organisms involved into account, which therefore must be adequately investigated during the relevant time interval (Wassmann et al., 2011).

Definition of environmental baselines is challenging, as the marine environment often has been impacted by human activities or climate change for many years (Hinz et al., 2011). Benthic foraminifera can be a helpful tool to reconstruct in-situ reference conditions. Benthic foraminifera are unicellular organisms (meiofauna, 45-1000 µm) living on top of and within the first centimeters of the seafloor sediment. Foraminifera are widely used as indicators for climatic and environmental changes and have a shell that fossilizes in the sediment, providing an archive of past changes. By studying live and fossilized foraminiferal assemblages in sediment cores, the method enables reconstruction of pre-impacted reference conditions in already impacted areas, present-day ecosystem impact, and monitoring of ecosystem recovery after environmental pressure has diminished (Dolven et al., 2013; Polovodova Asteman et al., 2015). Additionally, studying foraminifera in sediment cores will provide multiannual to decadal-scale records of natural environmental change, providing a record of the area's natural variability. Recent development and standardization of new bio-monitoring methods based on foraminifera (Aagaard-Sørensen et al., 2017; Alve et al., 2016; Barras et al., 2014; Bouchet et al., 2012; Schönfeld et al., 2012), has led to consideration to include the foraminiferal method in the EU legislation. Additionally, the Norwegian authorities now recommend using foraminifera to reconstruct in situ environmental baseline conditions (Veileder02:2013, 2015).

The main objective of this study is to determine the pre-impacted environmental baseline and natural variability of foraminiferal assemblages and sediment properties for the SW Barents Sea since 1800 CE. Variability in Atlantic Water inflow has a strong influence on the seafloor environment of the SW Barents Sea, as it transports both heat (Loeng and Drinkwater, 2007), nutrients (Knies and Martinez, 2009) and metals (e,g, AMAP, 1998; Junttila et al., 2014) toward the region. To establish reliable baselines for the area, it is therefore of importance to additionally improve our understanding of the variability in Atlantic Water inflow toward the Barents Sea. Five sediment cores were investigated following the pathway of Atlantic Water to the northeast through the Bjørnøyrenna trough (Fig. 1). Benthic foraminiferal assemblages, grain size distribution, total organic carbon and heavy metal concentrations were analyzed. An age model was obtained by the ^{210}Pb dating method. Our findings will serve as a robust dataset of baseline conditions and natural variability that can be used for future reference to monitor environmental impact of anthropogenic activities in the Barents Sea. This will be of great importance with the opening of new blocks for petroleum exploration in more northern and eastern parts of the Barents Sea (NorwegianPetroleumDirectorate, 2017). In addition, it will serve as baseline to monitor impact of other environmental change, including climate change and Atlantification of the Barents Sea (Wassmann et al., 2011).

2. Oceanography

Cores were collected in the glacially eroded Bjørnøyrenna trough (Andreassen et al., 2008) located in the Barents Sea (Fig. 1). The present day sedimentary environment is dominated by undisturbed silty

clay deposits (Wilson et al., 2011). Three main water masses prevail in the Barents Sea: Atlantic Water (AW), Arctic Water (ArW) and Coastal Water (CW) (Fig. 1). Additionally, a mixture of AW and ArW can form the local Barents Sea Water (BSW) (Hopkins, 1991), with temperatures around 0 °C and salinities of 34.4–35. CW (> 2ºC, < 34.7) (Loeng, 1991) is transported northwards along the Norwegian coast and is confined to the south western part of the Barents Sea. AW is characterized by higher salinities and temperatures (>35; >3 ºC) (Loeng, 1991). ArW enters the Barents Sea from the north and has low salinities (34.3 and 34.8) and temperatures (-1.5ºC), resulting in seasonal formation of sea ice (Loeng, 1991). In the Barents Sea, dense AW descends under the colder ArW, resulting in the formation of the oceanic Arctic Front (AF). At the AF, high nutrient availability results in increased primary production, especially just south of the front (Sakshaug and Slagstad, 1992). The maximum sea ice extent occurs between February and March, while the Barents Sea might be completely ice free from late summer to autumn (Vinje and Kvambekk, 2001). The inflow of AW, and hence salinity and heat, as well as variations in sea ice extent and location of the AF, have large effects on the Barents Sea ecosystem (Loeng and Drinkwater, 2007).

3. Material and Methods

3.1 Samples

Cores were collected at 5 locations in the SW Barents Sea following the pathway of AW up north. Core locations were chosen in basins at deeper water depths where sediment accumulation rates are expected to be highest, improving chances of undisturbed cores with a high temporal resolution (Fig. 1, Table 1). Cores were collected during different years, i.e. July 2012 (893, 897, 902 and 903) and June 2015 (core 993) (Table 1). Sediment cores were retrieved by a multi-corer. Six sediment cores maximum half a meter apart from one another, were retrieved simultaneously with one multi-corer cast. Three sediment cores per station were used in this study (Table 1). The cores were sliced in sub-samples at 1 cm intervals down to 20 cm (Table 1) directly after recovery. A rose Bengal ethanol mixture (1 g/1 L ethanol 95%) was added to the top 5 cm of the cores intended for foraminiferal analyses to stain living cytoplasm to distinguish between live (stained) and fossil fauna (Walton, 1952). Staining of the samples was allowed for a minimum of two weeks (Lutze and Altenbach, 1991). All samples were stored cool (<5°C) and were freeze-dried before further analyses, apart from those stained with rose Bengal.

3.2 Sediment properties

The grain size measurements were carried out with a Laser Diffraction Particle Size analyser (Beckman Coulter LS 13320). Just before analyses, a drop of Calgon solution was added to the samples which were then placed in an ultrasound bath to remove flocculated grains. Each sample was analyzed three times and the average grain-size distribution was calculated.

Total organic carbon (TOC) content was determined using a Leco CS-744 induction furnace. Inorganic carbon was removed from the bulk sediment sample with 10% HCl prior to measurement.

Metal concentrations were analyzed by UniLab AS, Fram Centre in Tromsø, Norway. Samples were homogenized and sieved through a 2µm mesh size before being decomposed with nitric acid. Concentrations of barium (Ba), cadmium (Cd), copper (Cu), chromium (Cr), lead (Pb), titanium (Ti) and zinc (Zn) were analyzed using inductively coupled plasma atomic emission spectroscopy (ICP-AES) or inductively coupled plasma sector field spectroscopy (ICP-SFMS), depending on the concentrations of the metals in the samples following Mannvik et al., (2011). Concentrations of Mercury (Hg) were measured with atomfluorescence (AFS) following Mannvik et al., (2011).

3.3 Foraminiferal counts

Fossil and live faunas were studied in the 100 µm to 1 mm fraction, to enable comparison to previous studies from the area (Dijkstra et al., 2015; Hald and Steinsund, 1992; Saher et al., 2012; Wilson et al., 2011). For the live fauna, only specimens with a bright stain inside more than half of the chambers were considered to be living at the time of sampling (de Stigter et al., 1998; de Stigter et al., 1999). We aimed to identify a minimum of 300 specimens per sample (Schönfeld et al., 2012). However, due to low foraminiferal density in some samples this number was not always reached, especially not for the live assemblages. Statistical studies based on a large number of paleo-ecological datasets, demonstrated that a sample size ranging between 25 and 60 specimens effectively produced the same multivariate result as samples based on a larger amount of specimens (Forcino, 2012; Forcino et al., 2015). Therefore, in case of samples with low amounts of specimens, we considered identification of 60 specimens as a minimum to consider the identified specimens as representative of the assemblage.

Foraminifera were identified following the generic classification of Loeblich and Tappan (1987) and the holotype descriptions in the Ellis and Messina catalogues (Ellis and Messina, 1940–1978). Nomenclature follows largely the accepted species names published in the WoRMS database (Mees et al., 2015). Some species were grouped during identification, see Supplementary data B for taxonomic notes.

Flux was calculated following the method of Ehrmann and Thiede (1985):

*flux (#/cm^2*yr) = absolute abundance (#/g) x bulk density (g/cm^3) x SAR (cm/yr)*

where SAR is the sediment accumulation rate. Bulk density was calculated from the sediment water content and porosity, with assumption of an average mineral density of 2.45 g/cm^3. Sediment accumulation rates were calculated at 1 cm resolution via ^{210}Pb datings (see below).

4. ^{210}Pb dating and age model

The sediments were ^{210}Pb dated on a 1 cm interval resolution at GEL Laboratories in Charleston, USA. Ages in this paper are based on the Constant Rate of Supply (CRS) (Appleby and Oldfield, 1992) model following the approach of Junttila et al., (2014). All ages were calculated for mid-layer depths (Fig. 2). In all cores, the excess ^{210}Pb fell to zero before 20 cm core depth (Fig 2; Table 2). Below these core depths, ages were determined by extrapolation, using the sediment accumulation rates (SAR) of the last

datable core interval. As the main objective of the study is to reconstruct natural variability in the Barents Sea since 1800 CE, we discard samples older than ca.1800 CE (Fig. 2). The excess ^{210}Pb depth profile of core 902 shows an increase in excess ^{210}Pb between 5-9 cm core depths, compared to the interval above, indicating a possible disturbance of the core. Therefore care should be taken interpreting the ages and sedimentation rates assigned to this core interval, i.e. 1967-1995 CE.

The average sediment accumulation rates per core, based on the Constant Initial Concentrations model, are: 0.94 mm/year (core 993), 0.67 mm/year (core 893), 1.2 mm/year (core 897), 1.8 mm/year (core 902) and 2.0 mm/year (core 903). Hence sediment accumulation rates increase towards the north of the transect.

5. Results

5.1 Grain size analyses and TOC

The cores are dominated by the fine fraction, i.e. silt (2-63 µm) and clay (< 2 µm) (Table 3; Fig. 3). The fine fraction has average values between 78 to 90 % of the bulk sample material in all cores. In core 993, 897 and 903, the sand content increases towards the core top, while in the other cores the opposite trend is observed (Fig. 3).

TOC values are highest in core 903 (average value 2.1%) and lowest in core 993 (0.6 %) (Fig. 3). Core 893 (average 1.0 %) and 897 (1.1%) show increased TOC contents towards the present. Core 993 shows a decreasing trend until 7.5 cm core depth, hereafter the TOC content increases towards the present. Core 902 (2.0%) and 903 (2.1%) have a relatively high but stable TOC content.

5.2 Heavy metal concentrations

Metal concentration ranges and average values are summarized in Table 3 (Supplementary data A). The average concentration of Ba, Cr, Pb, Zn and Ti are highest in core 893, while average concentrations of Cd and Cu are highest in core 903. The average concentration of Hg was highest in core 902. Core 897 overall exhibits lowest metal concentrations, apart from Ba, Hg and Pb, which show lowest average concentrations in core 993.

5.3 Live fauna

Rose Bengal stained specimens were observed in the top 5 cm of cores 893, 897, 902 and 903, indicating that these specimens were alive during core taking. In core 993, stained specimens were only observed in the top cm (Fig. 4; Supplementary data B). Counts from the individual top 5 cm samples were summed per core, as they are thought to present the entire live fauna during core retrieval at the core location (Fig. 4).

The amount of live specimens per ml is high in core 993, i.e. 9 specimens per ml sediment. In the other cores, the amount of live specimens per ml fluctuates between 1.2 and 2.1 #/ml (Fig.4). The number of observed live taxa is highest in core 902, 26 species, and lowest in core 993, 14 species (Fig. 4).

Amongst the live agglutinants *Adercotryma glomerata, Cribrostomoides* spp., *Reophax* spp., and *Trochammina* spp. were most abundant (Supplementary data B). Amongst the calcareous taxa, *Melonis barleeanus* and *Epistominella nipponica* are most abundant. Other species that reach relative abundances of > 10 % in at least one sample include *Buccella* spp., *Cassidulina neoteretis, Cibicides lobatulus, Pullenia bulloides* and *Trifarina angulosa* (Supplementary data B).

5.4 Fossil fauna

In total, 58 different taxa were identified; 50 calcareous and 8 agglutinated taxa (Supplementary data B). As most of the taxa were calcareous species, the number of species of the total fossil assemblage (agglutinated + calcareous taxa) and calcareous assemblage show similar trends. The number of agglutinated taxa is relatively stable throughout the cores (Fig. 5). Total fossil fluxes, representing the fossil fauna including both agglutinated and calcareous species, (Fig. 5) show maximum core values between 1.05 (core 897) and 23 #/cm^2/year (core 993); minimum fluxes vary between 0.004 (core 902) and 0.9 #/cm^2/year (core 993) (Figure 5). The average total fossil flux is highest in core 993 (mean = 7.4 #/cm^2/year) and lowest in core 893 (mean = 0.2 #/cm^2/year). Core 897, 902 and 903 have average total fossil fluxes of 0.3, 0.9, and 0.7 #/cm^2/year respectively. In all cores the flux increases towards present day, albeit that in core 903, fluxes decrease until 1951 CE (10.5 cm core depth), where after the flux increases towards the present. Additionally, core 993, 893 and 897 show low and stable fluxes before ca. 1900 CE, where after the flux doubles and starts to increase towards the present. A similar trend is observed in core 902, albeit that fluxes increase after 1940 CE. As calcareous taxa make up the majority of the assemblage, the calcareous flux is close to the total fossil flux both in quantity and trend. Agglutinated fluxes decreases rapidly down-core.

Downcore loss of fossil agglutinants is a well-known phenomenon (Murray, 2006 and references therein). Due to the poor downcore preservation of agglutinated taxa, the fluxes and relative abundances below are calculated with exclusion of all agglutinated taxa (Harloff and Mackensen, 1997; Mackensen et al., 1990). The down core trends of agglutinants will not be discussed in further detail. However, *Trochammina* spp., *Reophax* spp., and *Cribrostomoides* spp., are the most frequently observed agglutinated taxa (Supplementary data B).

Taxa with relative abundances of >5% in at least one sample in each core are shown in Fig. 4 and 6. Changes in individual species fluxes (Fig. 6) largely correspond to changes in either total calcareous flux or the relative abundance of the corresponding species. Further mention of individual species flux will therefore be limited to where they show differences and/or are relevant to the discussion.

Core 993 is dominated by *C.neoteretis* (mean relative abundance = 24%) with sub-dominance of *C.lobatulus* (17%) (Fig. 6). Other common species include *E.nipponica* and *C.laevigata*, both increasing in abundance towards the present. *C.lobatulus, Buccella* spp., *Islandiella* spp., *Nonionella auricula* and *Elphidium clavatum* (previously referred to in literature as *E. excavatum* forma *clavata*, see taxonomic

notes) decreases in abundance towards the present, albeit that their fluxes increases (Fig. 6). *M.barleeanus* decreases in abundance until ~1990 CE, while *Nonionellina labradorica* disappears after 1850 CE and appears again after 1950 CE (Fig. 6).

M.barleeanus dominates in core 893 (33%) with a sub-dominance of *E.nipponica* (11%) and *C.neoteretis* (12%). From 1800 to 1880 CE total calcareous flux and species fluxes are low, and abundances of *C.lobatulus, E.nipponica, C.neoteretis, C.reniforme* and *Islandiella* spp. are relatively high. Between 1800-1980 CE, *C.lobatulus, Buccella* spp., *C.neoteretis* and *C.reniforme* show high relative abundances and fluxes. After 1980 CE an overall increase in total calcareous flux and species fluxes is observed, and *M.barleeanus, E.nipponica, C.laevigata* and *Islandiella* spp. show high relative abundances (Fig. 6).

M.barleeanus dominates in core 897 (29%) with a sub-dominance of *E.nipponica* (11%) and *C.reniforme* (13%). From 1800 to 1920 CE, fluxes are low, while relative abundances of *C.lobatulus, M.barleeanus, Buccella* spp., *C.laevigata, Islandiella* spp. and *E.clavatum* are relatively high. Between 1920-1980 CE fluxes increase. The relative abundance of *Buccella* spp. remain high, while *C.reniforme, Islandiella* spp., and *E.clavatum* peak in this interval. After 1980 CE, *M.barleeanus, C.laevigata, C.neoteretis, N.labradorica* and *N.auricula* become more abundant (Fig. 6).

In core 902 (29%) and 903 (28 %) *Buccella* spp. is the dominating taxon. Other sub-dominant species in these cores are *M.barleeanus* (15% and 12% respectively) and *Islandiella* spp. (15% and 16% respectively). Before 1920 CE core 902 contains a low amount of foraminifera, and the assemblage is dominated by *Buccella* spp. (29%) (Fig. 6; Appendix B). Other sub-dominant species in this interval are *M.barleeanus* (15%) and *Islandiella* spp. (15%). The relative abundance of *Buccella* spp. drops after 1920 CE when total calcareous flux and species fluxes increase and other species start to occur in the assemblage, i.e. *M.barleeanus, E.nipponica, C.neoteretis, C.reniforme, E.clavatum* and both *Nonionella* species increase. After 1980 CE, these species continue to be more abundant, apart from *E.clavatum* which abundance decreases towards the present (Fig. 6). *C.laevigata* is more or less absent apart from one sample in the top of the core. For core 903, *Buccella* spp., *E.nipponica* and *M.barleeanus*, have high abundances between 1880 and 1970 CE while the flux is low. *C.lobatulus, Islandiella* spp., *E.clavatum* and *N.labradorica* show the same trend, with high relative abundances before 1880 CE, a low in abundances between 1880-1970 CE and high or a peak in relative abundance from 1970 towards the present. *C.laevigata* is not observed in the assemblage of core 903, *C.neoteretis* only appears in the very top of the core, while *E.nipponica* has a low abundance compared to what is observed in the other cores, with increased abundance after 1970 CE (Fig. 6).

6. Discussion

6.1. Metal concentrations and anthropogenic influence

Most metal concentrations measured in the cores correspond to background levels (level I) according to Norwegian sediment quality classification (Bakke et al., 2010). Some intervals are classified as level II,

corresponding to concentrations with no toxic effects, i.e. Cr concentrations in core 893, Hg concentrations in core 902, Cd concentrations in all cores but 897 (Fig.3; Supplementary data A). Similar concentrations were measured in surface sediments and sediment cores from Ingøydjupet and the adjacent Tromsøflaket (Dijkstra et al., 2013; Dijkstra et al., 2015). These environmental classes are not developed for Ba and Ti. However, Ba concentrations fall within the same range as observed in the nearby Ingøydjupet trough (< 200 mg/kg) (Dijkstra et al., 2015), and concentrations in the top of the cores do not significantly exceed concentrations measured at 1800 CE. Titanium concentration do not exceed values observed in nearby baseline studies, i.e. <1410 mg/kg (Dijkstra et al., 2015). It should be noted that the down core distribution of Cd in all cores show a remarkable pattern compared to the other metals, showing different trends than the other metals or peaks of elevated concentrations (Fig. 3). Previous studies from the area reported similar patterns in Cd concentrations (Dijkstra et al., 2015; Jensen et al., 2009), which was attributed to post depositional processes (Kjeldsen and Christensen, 1996). Therefore, we do not consider its down core distribution pattern as reliable indicator of past metal concentrations and input.

As all metal concentrations are classified to levels of no effect, impact of the metal concentrations on foraminifera is not expected. Non-impacted baseline faunas have been reported in a Norwegian Fjord (Polovodova Asteman et al., 2015) and the nearby Ingøydjupet trough (Dijkstra et al., 2013; Dijkstra et al., 2015) where metal concentrations were of levels reported in the Bjørnøyrenna cores (Fig. 3).

We observed visual similarities (Fig. 3) in down core distribution patterns between the metal concentrations and TOC and/or clay. In cores 993, 893 and 897, concentrations of Ba, Cr, Cu, Zn and Ti show a similar down core pattern to one another, and to either TOC or clay (Fig. 3). Clay and TOC particles generate a larger metal binding potential of the sediments (Horowitz, 1991; Kennedy et al., 2002). The similarity between the profiles of Ba, Cr, Cu, Zn and Ti and either TOC or clay (Fig. 3) therefore suggests that variability in the metal concentrations at sites 993, 893 and 897 can be contributed to the natural variability in local sediment properties and thus capability of metal uptake, rather than variability in input. The down core distribution of Pb and Hg on the other hand, often show a similar pattern, but a different temporal trend than the other metals (Fig. 3). Additionally, they often show similarity to the down core profile of TOC concentrations, especially after ca. 1900 CE. As increased TOC values are associated with enhanced inflow of AW (Knies and Martinez, 2009), we attribute the variability in the concentration of Hg and Pb to the variability in AW inflow, with AW serving as transporting agent of the metals. A similar pattern has been observed in previous studies (AMAP, 1998; Jensen et al., 2009; Junttila et al., 2014). Hence, the down core variability in Hg and Pb concentrations can be considered as indicator of (natural) variability in AW inflow.

In both core 902 and 903, Ba, Cr, Cu, Zn and Ti, show similar trends, as do Hg and Pb. However, the down core distribution in element concentration shows less similarity to either TOC or clay (Fig. 3). It should be noted that the TOC content in cores 902 and 903 is almost twice as high as in the more

309 southern cores (993, 893, 897). Similar trends in TOC have been observed in surface samples by Knies
310 and Martinez (2009), attributable to the differences in oceanography along the transect. The northern
311 core sites, are located close to the AF (Fig. 1). The TOC content of these southern sites (993, 893 and
312 897) will therefore be mainly composed of marine organic material originating from the nutrient rich
313 AW (Knies and Martinez, 2009), while the TOC at core sites 902 and 903 additionally will experience
314 TOC input from the high productivity at the AF (e.g. Sakshaug and Slagstad, 1992). This explains the
315 higher TOC concentrations at core location 902 and 903 (Table 3). These high TOC concentrations will
316 'overwrite' any potential signal between TOC originating from AW and metals transported by AW. This
317 is supported by the fact that concentrations of metals are not significantly higher than at the southern
318 sites, despite the potentially higher metal binding capacity of the sediments.
319 Sediment cores from nearby locations in Ingøydjupet (Dijkstra et al., 2015; Jensen et al., 2009), show
320 an increase in concentrations of Hg and Pb after ~1960 CE, which coincides with the onset of emission
321 of leaded gasoline into the atmosphere (AMAP, 2005). In our study, increased Pb concentrations are
322 observed from ca. 1960 CE (Fig. 3), albeit that an increase in concentrations started earlier on in most
323 cores, for natural reasons discussed above. Hg concentrations (further) increase in core 897 around 1960
324 CE, while in cores 993 and 902 the increase is initiated slightly later. Although Hg and Pb concentrations
325 could be correlated with increased TOC or clay content in core 993, 893 and 897 (see discussion above),
326 it could very well imply an anthropogenic signal from an atmospheric source as well.
327 Overall, it can be concluded that the down core distribution of metal concentrations can be attributed to
328 (natural) variability of the sediment properties (clay and TOC) and natural changes in AW inflow
329 serving as transport agent for Hg and Pb. Hence, the reconstructed range in down core metal
330 concentrations (Table 3), corresponding to background values (Bakke et al., 2010), can be considered
331 to reflect the areas environmental baseline and natural variability.
332
333 **6.2. Regional trends in foraminiferal assemblages**
334 The most abundant species and their environmental interpretations are summarized in Table 4 (see
335 references therein).
336 The average relative abundances of the most abundant species of the live and fossil assemblages show
337 a clear geographic trend along the Bjørnøyrenna transect (Fig. 4). Overall, *C.neoteretis, E.nipponica,*
338 *C.laevigata* and *N.auricula*, associated with relatively warmer temperatures and/or AW influenced
339 bottom waters, diminish along the transect up north. *Buccella* spp., *Islandiella* spp., *E.clavatum* and *N.*
340 *auricula*, associated with lower bottom water temperatures and proximity to the AF, become more
341 abundant northeast along the transect. This can be explained by the decreasing seawater temperatures
342 toward the northern and central part of the Barents Sea corresponding to the known distribution of water
343 masses, with warm AW in the south and central part, and cool ArW in the north of Bjørnøyrenna (Fig.
344 1; Loeng, 1991). The abundance of live and fossil *C.reniforme* is highest in the middle part of the
345 transect. The species thrives in colder (~2°C), yet relative saline conditions, indicating that the middle

part of the transect experiences influence of both AW and ArW. The higher abundance of both live and fossil epifaunal species *C.lobatulus* in station 993 is attributed to coarse grain sizes at this station,. More preferable conditions for epifaunal species in station 993 is also suggested by absence of live specimens below 1 cm sediment depth. The high abundance of live and fossil *M.barleeanus* and *N.auricula* in station 893 and 897 might indicate high amounts of degraded organic matter in this part of the Bjørnøyrenna trough. The slightly lower abundance of *M.barleeanus,* towards the north of the transect i.e. 902 and 903 (Fig. 4), suggests that nutrient availability at these sites might predominantly originate from fresh phytodetritus produced at the high productive AF.

Based on these trends along the studied transect, we divided the dominating foraminiferal species into two groups (Table 4): (a) warm (Atlantic) associated species including *C.laevigata, E.nipponica, C.neoteretis, M.barleeanus* and *N.auricula*; (b) cool (Arctic) associated species including *Buccella* spp., *E.clavatum, Islandiella* spp., *N.labradorica* and *C.reniforme* (Fig.6B).

6.3 Temporal trends

Effects of natural environmental changes will be superimposed on anthropogenic induced changes. The applicability of an environmental baseline must therefore always take the natural variability of the processes or organisms involved into account during the relevant time interval (Wassmann et al., 2011). This natural variability might include changes in oceanography, food availability, and decadal scale climatic variability. As the low metal concentrations in the studied cores, are not expected to influence the foraminiferal assemblages, the down core foraminiferal assemblages will provide a high resolution record of such natural variability. The down core foraminiferal distribution, together with the live assemblages discussed in 6.2, are therefore considered to reflect the areas' environmental baseline and its natural variability.

Below we discuss temporal trends in benthic foraminiferal assemblages in relation to variability of AW inflow into the area, as its variability is one of the main drivers of natural environmental change in the Barents Sea on a (multi-)decadal time scale. Atlantic Water is an important distributor of heat into the Barents Sea (Loeng and Drinkwater, 2007). Additionally, the nutrient rich AW intensifies primary productivity and increases the vertical flux of marine organic material, resulting in elevated total organic carbon content (TOC) of the seafloor sediment (Knies and Martinez, 2009) providing an important food source for foraminifera (Loubere and Fariduddin, 1999). At the same time, Atlantic Water transports metals from the south into the Barents Sea (AMAP, 1998; Dijkstra et al., 2015; Junttila et al., 2014). Elevated sediment TOC generates a larger metal binding potential of the sediments resulting in larger sediment uptake of metals (Horowitz, 1991; Kennedy et al., 2002). The variability of inflow of AW into the Barents Sea thus has both a direct (inflow of metals) and indirect effect (binding of metals to organic matter) on sediment metal concentrations, and simultaneously influences the foraminiferal assemblages (food source). This results in a complex interplay, and can cause false positive correlations between foraminiferal abundance (flux) and metal concentrations (Dijkstra et al., 2015).

Accordingly, four parameters are considered as (indirect) indicators of AW presence and/or variability in AW inflow:

(1) Presence of the warm associated foraminiferal species, as AW is the main distributor of heat (Loeng and Drinkwater, 2007).

(2) Increased total calcareous fluxes, as AW indirectly provides a food source for the benthic environment (Loubere and Fariduddin, 1999).

(3) Elevated TOC content, as a result of the increased vertical flux of marine organic matter (Knies and Martinez, 2009).

(4) Elevated Hg and Pb concentrations, as AW is a transport agent of Hg and Pb (see discussion in 6.1).

Based on the assemblages (Table 4) and physical parameters, the cores have been divided into three intervals: ~1800-1900 CE, ~1900-1980 CE, ~1980-present (Fig. 6D). The boundary between the different time intervals differs from core to core with an offset of 10-30 years, attributable to uncertainties in the age model or a delayed effect of oceanographic changes between the sites due to their different geographical location (see below). The study area is divided into two regions: (a) SW cores 993, 893 and 897, mainly influenced by variability in AW inflow; (b) NE cores 902 and 903, influenced by both variability in AW inflow and proximity to the AF (Fig. 6).

Environmental interpretation of the main foraminiferal species and corresponding references are summarized in Table 4.

Interval I: ~1800 to ~1900 CE

In the SW cores, 993, 893 and 897 fluxes are initially low indicating unfavorable conditions for foraminifera (Fig. 6). Higher abundances and species flux of the cold associated species indicate initially cold bottom waters (Table 4). However, presence of *C.neoteretis*, *E.nipponica* and *C.laevigata* additionally indicates influence of AW. The relatively high abundance of *C.lobatulus* in core 993 compared to its abundance in the other two SW cores, can be explained by the relatively high sand content of the core (Fig. 3). This indicates higher bottom current speeds at core location 993 than at the other SW sites. The same is observed for the other time intervals. The decline of *E.clavatum* and *N.labradorica* and overall increased total fluxes since ~1860 CE, reflect a shift from initially cool conditions with low food availability to warmer conditions (Fig. 6). Wilson et al., (2011) reported a similar shift at a closeby location in Bjørnøyrenna, which was correlated to the termination of the Little Ice Age (LIA). The cold conditions of the LIA (1500–1900 CE) are thought to be the result of a weak Atlantic Meridional Overturning Circulation, and reduced flow of AW towards the north (Trouet et al., 2011). Enhanced inflow of AW in our study area towards the termination of LIA is additionally supported by the gradual increase of both TOC and Pb towards ~1900 CE (Fig. 3).

Total calcareous fluxes are low in the NE cores 902 and 903. In these cores the relative abundance of *Buccella* spp. (mainly consisting of *B.frigida*) is high, (Fig. 6), and abundance and fluxes of the other

cold associated species (Table 4, Fig. 6) gradually increase, indicating Arctic conditions and proximity of the AF and/or sea ice edge. High TOC values (Fig. 3 and 6) support the proximity of the AF/sea ice edge, associated with high biological activity and fresh phytodetritus. Despite the high food availability, conditions were unfavorable for the foraminifera, as indicated by the overall low total calcareous fluxes. This might indicate (seasonal) presence of sea ice, which is supported by the relative high abundance of *Buccella* spp.. Historical records on the location of the sea ice edge, report its southernmost position between 1800-1900 CE (Vinje, 2001). Hald and Steinsund (1996) observed highest amounts of *Buccella* spp. when dissolution is common and calcareous foraminifera are rare. Hence the high abundance of this species, in combination with the low fluxes, might additionally indicate presence of corrosive ArW, creating unfavorable conditions for calcareous foraminifera and postmortem dissolution.

To summarize, during the 1800-1900 CE interval (Fig. 6 D), the assemblages in the SW part of the study area indicate AW influenced yet chilled conditions corresponding to the termination of the LIA. The assemblage in the NE part of the study area indicate colder Arctic conditions and proximity to the AF with potentially corrosive bottom waters.

Interval II: ~1900 to ~1980 CE

In the SW cores a further increase in total calcareous fluxes is observed during interval II, indicating increased delivery of nutrients towards the core site, which is supported by the increasing TOC content (Fig. 6). In core 993, the higher abundance of *E.nipponica* indicates further warming of the water mass. For core 893, the higher TOC and fluxes (Fig. 6) indicate influence of AW, albeit with relatively low temperatures as indicated by the increased abundance of *C.neoteretis* and *C.reniforme* (Fig. 6). The increase of Hg and Pb at site 993 and 893 since ~1900 CE (Fig. 3) supports increased inflow of AW. This is additionally supported by increased relative abundances of *M.barleeanus* in core 893. In core 993, the abundance of the species follows the overall decline of clay (Fig. 6) and high abundance of *C.lobatulus*, all attributable to higher bottom current speeds. We therefore hypothesize that the intensified inflow of AW around 1900 CE was accompanied by increased bottom current speeds at core location 993. In core 897, the relatively high abundance of cold associated species, in combination with presence of warm associated species, indicates a mixture of AW and ArW, i.e. BSW. The latter indicates less influence of AW at site 897, compared to the previous time interval (Fig. 7D).

For core 902, the increased total calcareous flux and relative abundance of both *E.nipponica* and *C.neoteretis* around 1900 CE suggest presence of chilled AW. The overall increase of fluxes suggests enhanced food availability, and hence inflow of AW. Simultaneously cool (and fresh) conditions are supported by higher relative abundances of the cold associated species (Fig. 6) and near absence of *C.laevigata*. The presence of both cold species and increased Atlantic species are therefore interpreted to reflect presence of BSW. The observed signal of enhanced Hg and Pb concentration with increased AW inflow, as observed in the SW cores, is not visible for core 902 in interval II (Fig. 3). This might be due to the high productivity at the proximal AF masking the correlation as discussed in chapter 6.1.

The low fluxes and high abundance of *Buccella* spp. in core 903 (Fig. 6) indicate similar cold Arctic conditions, and potentially corrosive bottom waters as in interval I, i.e. dominance of ArW, proximity of the AF and potentially presence of (seasonal) sea ice. The (time) offset between core 902 and 903 can be related to a delayed inflow of AW to core site 903. However, as the cores are relatively close (~60 km) the offset might also be caused by uncertainties in the age model.

The presence of warm associated species *E.nipponica*, albeit <4%, during the cold Interval II and I in core 903 is remarkable. *Epistominella nipponica* is morphologically identical to the temperature indifferent deep water species *Alabaminella weddellensis* (Saher et al., 2012), albeit that it has been observed at water depths corresponding to those found along the Bjørnøyrenna transect (Culver and Buzas, 1980; Saher et al., 2012). The species thrives on pulsed phytodetritus (Smart and Gooday, 1997; Sun et al., 2006). Presence of *Buccella* spp. and *N.labradorica* during this time interval also indicates pulsed phytodetritus (Fig. 6) originating from the AF. We therefore argue that *E.nipponica* either has similar environmental preferences as *A.weddelensis*, or *E.nipponica* was been misidentified in these intervals and actually represents the morphological similar *A.weddelensis* (i.e. pulsed phytodetritus).

Sea surface temperature records from the Kola peninsula (PINRO, 2013; Smedsrud et al., 2013) and Fugleøy-Bjørnøya transect (Ingvaldsen et al., 2002), as well as atmospheric temperature records from the Northern Hemisphere and Barents Sea (Ikeda, 1990; Rayner et al., 2003) report decadal scale climate variability between 1900-1980 CE. This natural variability is linked to the North Atlantic Oscillation, causing variable inflow of AW into the Barents Sea (Dickson et al., 2000; Goosse and Holland, 2005; Trouet et al., 2011). Decadal variability includes a cool period in the 1920s, warming from the mid 1920s to 1950s and cooling between the 1960s and 1970s (Ikeda, 1990; Rayner et al., 2003). A study from the nearby Ingøydjupet trough observed decadal variability in the total foraminiferal flux (Dijkstra et al., 2015). Assemblages of the SW cores register the two cooling periods as discussed above. The 1920s-1950s warming trend is however not clearly reflected by the assemblages. This might be due to the time resolution of cores, with no or only one sample within the time period. Decadal climatic variability is not observed in the NE cores. We attribute this to the northern location and influence from the ArW overruling the Atlantic signal.

Interval III: ~1980 to present

After ~1980 CE the increased abundance of warm associated species, and increasing total calcareous flux and TOC (Fig. 6), indicate enhanced inflow of AW and warming of the water mass in the SW cores, albeit with a delay of ~10 years for core 897. The increased abundances and species fluxes of *C.reniforme* and *Islandiella* spp. (Fig. 6), despite more warm AW influenced conditions, might therefore be due to increased salinity and nutrient availability, respectively. Increasing fluxes of *M.barleeanus* throughout the SW cores follow the increasing TOC content (Fig. 6) reflecting this increased food availability.

For the top part of NE core 902, the increase in total calcareous flux and abundances of *E.nipponica* and *C.neoteretis* suggest a further warming of the water mass and enhanced inflow of AW. The warming is supported by a decline in *Buccella* spp., *E.excavatum,* and *N.labradorica* (Fig. 6). Despite presence of AW, the abundance of *C.laevigata* is close to zero/absent, suggesting that conditions are too cold or fresh for the species. A similar trend is observed in core 903. Presence of both cold species and increased abumdance of Atlantic species suggest dominance of BSW. The observed signal of higher Hg and Pb concentration, with increased inflow of AW occurred, as observed in the SW cores, is to some extent visible in core 902 (Fig. 3). The Hg and Pb content of core 903 does not show a clear increase in concentrations after 1980 CE (Fig. 3), as a result of the high productivity of the front, diluting the Atlantic signal (see 6.1).

Overall, from ca.1980 CE towards present, all cores registered enhanced inflow of AW, transporting heat and nutrients into Bjørnøyrenna, resulting in both warming of the water mass and enhanced food availability for foraminifera. Warming of bottom waters and enhanced inflow of AW since 1980 CE is a well-documented phenomena in the Barents Sea (Bengtsson et al., 2004; Ingvaldsen et al., 2002). Atmospheric and sea surface temperature records show an overall increasing temperature and salinity in the Barents Sea region during the last 30-40 years (Carton et al., 2011; Furevik, 2001; Holliday et al., 2008; Rigor et al., 2000), as does a proxy record study from the Fram Strait (Spielhagen et al., 2011). Other foraminiferal studies from the area (Dijkstra et al., 2015; Risebrobakken et al., 2010; Wilson et al., 2011) indicated a similar warming. A study comparing live assemblages collected between 1962-1992 and 2005-2006 in the Barents Sea, reported an overall decrease of cold associated species and increase of AW associated species (Saher et al., 2012) as observed within the top of our records.

7. Summary and conclusion

Metal concentrations, sediment properties and benthic foraminiferal assemblages were investigated in five sediment cores along a SW-NE transect in the Bjørnøyrenna trough, to gain insight into the temporal natural variability of these parameters in addition to Atlantic Water inflow since 1800 CE. Additionally, the data set serves as an environmental baseline for monitoring potential future environmental impacts associated with petroleum industry activities and other anthropogenic activities in the area. With the expected increase in industrial activities, this will be of importance.

Overall, metal concentrations are considered to be of background/no effect levels (class I and II; Bakke et al., 2010), and are not expected to effect the foraminiferal assemblage. Down core changes in metal concentrations could be attributed to (natural) variability of the sediment properties (clay and TOC) and natural changes of Atlantic Water inflow serving as transport agent of Hg and Pb. An increase in Pb and Hg concentrations after 1960 CE in the SW part of the study area is potentially the only indication of an anthropogenic signal, associated to emission of leaded gasoline. Hence, the reconstructed range in down core metal concentrations and foraminiferal assemblage reflect the (non-impacted) environmental baseline and natural variability of the area.

The most common foraminiferal species could be divided into two groups. Warm associated species *E.nipponica, M.barleeanus, C.laevigata*, *C.neoteretis* and *N.auricula*, dominated the assemblages in the SW part (993, 893 and 897) of the transect and the upper part of all cores, and reflect the relatively warm conditions and high food flux associated to Atlantic Water inflow in Bjørnøyrenna. Cold, Arctic associated species *E.clavatum, N.labradorica, Buccella* spp., *C.reniforme* and *Islandiella* spp., dominated the assemblages in the NE part (902 and 903) of the transect, the lower parts of the cores from the SW part of the study area, and the entire time span of the two NE cores.

Four indicators of variability in Atlantic Water inflow were defined: (a) Presence of warm, Atlantic foraminiferal species; (b) Total calcareous fluxes; (c) Total organic carbon concentrations; (d) Elevated Hg and Pb concentrations. The cores could be divided into three time intervals accordingly, reflecting the natural variability in Atlantic Water inflow into Bjørnøyrenna since 1800 CE.

- 1800-1900 CE. The SW cores indicate increased inflow of cool Atlantic Water, in addition to warming of the water mass, corresponding to the termination of the Little Ice Age. The NE cores reflect presence of Arctic Water.
- 1900-1980 CE. The southernmost core 993 shows a further warming of the Atlantic Water mass, while core 893 and 897 show cooler conditions, indicating the presence of chilled Atlantic Water and Barents Sea Water, respectively. These cooler conditions towards the south indicate reduced inflow of Atlantic Water. Core 902 indicates presence of Barents Sea Water, while core 903 indicates Arctic Water.
- 1980 CE-present. All cores show enhanced inflow of Atlantic Water and warming of the water column. The SW sites are dominated by Atlantic Water, the NE sites by Barents Sea Water, indicating a northward retreat of the Arctic Front.

8. Acknowledgements

This study is part of the Barents Sea Drill Cuttings Research Initiative (BARCUT) - project (WP 3) funded by Eni Norway. ND additionally received funding from RDA Troms County. UiT co-funded shiptime. We thank the captain, crew and cruise engineers of *RV Helmer Hansen* for help during core recovery, in addition to all of the scientific participants of the GLACIBAR/EWMA 2012 cruise. Prof. Karin Andreassen is thanked for allowing us to use some of the cores obtained during this cruise. We are grateful to the reviewers providing constructive feedback on the manuscript.

9. References

Aagaard-Sørensen, S., Junttila, J., Dijkstra, N., 2017. Identifying past petroleum exploration related drill cutting releases and influences on the marine environment and benthic foraminiferal communities, Goliat Field, SW Barents Sea, Norway. accepted at Marine Pollution Bulletin.

Altenbach, A.V., Pflaumann, U., Schiebel, R., 1999. Scaling percentages and distributional patterns of benthic foraminifera with flux rates or organic carbon. Journal of Foraminiferal Research 29, 173-185.

Alve, E., Korsun, S., Schonfeld, J., Dijkstra, N., Golikova, E., Hess, S., Husum, K., Panieri, G., 2016. Foram-AMBI: a sensitivity index based on benthic foraminiferal faunas from North-East Atlantic and Arctic fjords, continental shelves and slopes. Marine Micropaleontology 122, 1-12.

AMAP, 1998. AMAP Assessment Report: Arctic Pollution Issues, in: Wilson, S.J., Murray, L.J., Huntington, H.P. (Eds.). AMAP, Oslo, Norway, p. xii + 265 pp.

AMAP, 2005. AMAP Assessment 2002: Heavy metal in the Arctic, in: Symon, C., Wilson, S.J. (Eds.), Arctic Monitoring and Assessment Programme (AMAP), Oslo, Norway, p. xvi+265.

Andreassen, K., Laberg, J.S., Vorren, T.O., 2008. Seafloor geomorphology of the SW Barents Sea and its glaci-dynamic implications. Geomorphology 97, 157-177.

Appleby, P.G., Oldfield, F., 1992. Applications of lead-210 to sedimentation studies, in: Ivanovich, M., Harmon, R.S. (Eds.), Uranium-Series Disequilibrium: Applications to Earth and Marine, and Environmental Problems. Clarendon Press, Oxford, UK, pp. 731-778.

Bakke, T., Källqvist, T., Ruus, A., Breedveld, G., Hylland, K., 2010. Development of sediment quality criteria in Norway. Journal Soils Sediments 10, 172-178.

Barras, C., Jorissen, F.J., Labrune, C., Andral, B., Boissery, P., 2014. Live benthic foraminiferal faunas from the French mediterranean coast: towards a new biotic index of environmental quality. Ecological Indiators 36, 719-743.

Bartels, M., Titschack, J., Fahl, K., Stein, R., Seidenkrantz, M.S., Hillaire-Marcel, C., Hebbeln, D., 2017. Atlantic Water advection vs glacier dynamics in northern Spitsbergen since early deglaciation. Clim. Past Discuss. 2017, 1-53.

Bengtsson, L., Semenov, V.A., Johannessen, O.M., 2004. The early twentieth-century warming in the arctic - a possible mechanism. Journal of Climate 17, 4045-4057.

Bouchet, V.M.P., Alve, E., Rygg, B., Telford, R.J., 2012. Benthic foraminifera provide a promising tool for ecological quality assessment of marine waters. Ecological Indicators 23, 66-75.

Carton, J.A., Chepurin, G.A., Reagan, J., Häkkinen, S., 2011. Interannual to decadal variability of Atlantic Water in the Nordic and adjacent seas. Journal of Geophysical Research Policy 116, C11035.

Culver, S.J., Buzas, M.A., 1980. Distribution of recent benthic foraminifera off the North American Atlantic Coast. Smithsonian Contributions to the Marine Sciences 6.

de Stigter, H.C., Jorissen, F., Van der Zwaan, G.J., 1998. Bathymetric distribution and microhabitat partitioning of live (Rose Bengal stained) benthic foraminifera along a shelf to deep sea transect in the southern Adriatic Sea. Journal of Foraminiferal Research 28, 40-65.

de Stigter, H.C., van der Zwaan, G.J., Langone, L., 1999. Differential rates of benthic foraminiferal test production in surface and subsurface sediment habitats in the southern Adriatic Sea. Palaeogeography, Palaeoclimatology, Palaeoecology 149, 67-88.

Dickson, R.R., Osborn, T.J., Maslowski, W., 2000. The arctic ocean response to the north Atlantic oscillation. Journal of Climate 13, 2671-2696.

Dijkstra, N., Junttila, J., Carroll, J., Hald, M., Elvebakk, G., Godtliebsen, F., 2013. Living benthic foraminiferal assemblages and their relationship to grain size and element concentrations in surface sediments of the Ingøydjupet-Tromsøflaket region, southwestern Barents Sea. Marine Environmental Research 92.

611 Dijkstra, N., Junttila, J., Husum, K., Carroll, J., Hald, M., 2015. Natural variability of benthic foraminiferal
612 assemblages and metal concentrations during the last 150 yrs in the Ingøydjupet trough, SW Barents Sea. Marine
613 Micropaleontology 121, 16-31.

614 Dolven, J.K., Alve, E., Rygg, B., Magnusson, J., 2013. Defining past ecological status and in situ reference
615 conditions using benthic foraminifera: A case study from the Oslofjord, Norway. Ecological Indicators 29, 219-
616 233.

617 Ehrmann, W.U., Thiede, J., 1985. History of Mesozoic and Cenozoic sediment fluxes to the North Atlantic Ocean.
618 Contributions to Sedimentology 15, 1-109.

619 Ellis, B.E., Messina, A.R., 1940–1978. Catalogue of Foraminifera American Museum of Natural History, New
620 York.

621 Forcino, F.L., 2012. Multivariate assessment of the required sample size for community paleoecological research.
622 Palaeogeography, Palaeoclimatology, Palaeoecology 315-316, 134-141.

623 Forcino, F.L., Leighton, L.R., Twerdy, P., Cahill, J.F., 2015. Reexamining Sample Size Requirements for
624 Multivariate, Abundance-Based Community Research: When Resources are Limited, the Research Does Not Have
625 to Be. PLoS One 10, 1-18.

626 Furevik, T., 2001. Annual and interannual variability of Atlantic Water temperatures in the Norwegian and Barents
627 Seas: 1980–1996. Deep Sea Research Part I: Oceanographic Research Papers 48, 383–404.

628 Gooday, A.J., Lambshead, P.J.D., 1989. Influence of seasonally deposited phytodetritus on benthic foraminiferal
629 populations in the bathyal northeast Atlantic: the species response. Marine Ecology Progress Series 58, 53–67.

630 Goosse, H., Holland, M., 2005. Mechanisms of decadal Arctic variability in the Community Climate System
631 Model CCSM2. Journal of Climate 18, 3552-3570.

632 Hald, M., Steinsund, P.I., 1992. Distribution of surface sediment benthic foraminifera in the southwestern Barents
633 Sea. Journal of Foraminiferal Research 22, 347-362.

634 Hald, M., Steinsund, P.I., 1996. Benthic foraminifera and carbonate dissolution in surface sediments of the
635 Barents-and Kara Seas, in: Stein, R., Ivanov, G.I., Levitan, M.A., Fahl, K. (Eds.), Surface sediment composition
636 and sedimentary processes in the central Arctic Ocean and along the Eurasian Continental Margin pp. 285-307.

637 Hald, M., Korsun, S., 1997. Distribution of modern benthic foraminifera from fjords of Svalbard, European Arctic.
638 Journal of Foraminiferal Research 27 27, 101-122.

639 Harloff, J., Mackensen, A., 1997. Recent benthic foraminiferal associations and ecology of the Scotia Sea and
640 Argentine Basin. Marine Micropaleontology 31, 1-29.

641 Hinz, H., Capasso, E., Lilley, M., Frost, M., Jenkins, S., 2011. Temporal differences across a bio-geographical
642 boundary reveal slow response of sub-littoral benthos to climate change Marine Ecological Progress Series 423,
643 69-82.

644 Holliday, N.P., Hughes, S.L., Bacon, S., Beszczynska-Möller, A., Hansen, B., Lavin, A., Loeng, H., Mork, K.A.,
645 Osterhus, S., Sherwin, T., Walczowski, W., 2008. Reversal of the 1960s to 1990s freshening trend in the northeast
646 North Atlantic and Nordic Seas. Geophysical Research Letters 35, L03614.

647 Hopkins, T.S., 1991. The GIN Sea — a synthesis of its physical oceanography and literature review 1972-1985.
648 Earth-Science Reviews 30, 175-318.

649 Horowitz, A.J., 1991. A Primer on Sediment–Trace Element Chemistry. Lewis Publishers Ltd., Chelsea.

650 Ikeda, M., 1990. Decadal oscillations of the air-ice-ocean system in the Northern Hemisphere. Atmosphere-Ocean
651 28, 106-139.

652 Ingvaldsen, R., Loeng, H., Asplin, L., 2002. Variability in the Atlantic inflow to the Barents Sea based on a one-
653 year time series from moored current meters. Continental Shelf Research 22, 505-519.

Jennings, A.E., Weiner, N.J., Helgadottir, G., Andrews, J.T., 2004. Modern foraminiferal faunas of the southwestern to northern Iceland Shelf; oceanographic and environmental controls. Journal of Foraminiferal Research 34, 180-207.

Jensen, H.K.B., Boitsov, S., Finne T. E., Klungsøyr, J., Knies, J., 2009. Physical and chemical traces of anthropogenic influence at the seabed and in the sediments in Ingøydjupet, Southern Barents Sea. Norwegian Journal of Geology 89, 101-108.

Junttila, J., Carroll, J., Husum, K., Dijkstra, N., 2014. Sediment transport and deposition in Ingøydjupet, SW Barents Sea. Continental Shelf Research.

Kennedy, M.J., Peaver, D.R., Hill, R.J., 2002. Mineral surface control of organic carbon in black shale. Science 295, 657-660.

Kjeldsen, P., Christensen, T.H., 1996. Kemiske stoffers opførsel i jord og grundvand, Prosjekt om jord og grundvand fra Miljøstyrelsen, nr. 20. DTU, Copenhagen, p. 507.

Knies, J., Martinez, P., 2009. Organic matter sedimentation in the western Barents Sea region: Terrestrial and marine contribution based on isotopic composition and organic nitrogen content. Norwegian Journal of Geology 89, 79-89.

Korsun, S., Hald, M., 1998. Modern Benthic Foraminifera off Novaya Zemlya Tidewater Glaciers, Russian Arctic. Arctic and Alpine Research 30, 61-77.

Korsun, S., Hald, M., 2000. Seasonal dynamics of benthic foraminifera in a glacially fed fjord of Svalbard, European Arctic. Journal of Foraminiferal Research 30, 251–271.

Linke, P., Lutze, G.F., 1993. Microhabitat preferances of benthic foraminifera - a static concept or a dynamic adaptation to optimize food acquisition? Marine Micropaleontology 20, 215-234.

Loeblich, A.R., Tappan, H., 1987. Foraminiferal genera and their classification. Van Nostrand Reinhold Co, New York.

Loeng, H., 1991. Features of the physical oceanographic conditions of the Barents Sea. Polar Research 10, 5-18.

Loeng, H., Drinkwater, K., 2007. An overview of the ecosystems of the Barents and Norwegian Seas and their response to climate variability. Deep Sea Research Part II: Topical Studies in Oceanography 54, 2478-2500.

Loubere, P., Fariduddin, M., 1999. Benthic foraminifera and the flux of organic carbon to the seabed, in: Sen Gupta, B.K. (Ed.), Modern Foraminifera. Kluwer Academic Publisher

UK, pp. 181-199.

Lutze, G.F., Altenbach, A., 1991. Technik und Signifikanz der Lebendfarbung benthischer Foraminiferen mit Bengalrot. Geologisches Jahrbuch 128, 251-265.

Mackensen, A., Hald, M., 1988. Cassidulina teretis Tappan and C.laevigeta d'Orbigny; their modern and late Quaternary distribution in northern seas. Journal of Foraminiferal Research 18, 16-24.

Mackensen, A., Sejrup, H.P., Jansen, E., 1985. The distribution of living benthic foraminifera on the continental slope and rise of southwest Norway. Marine Micropaleontology 9, 275-306.

Mackensen, A., Grobe, H., Kuhn, G., Fütterer, D.K., 1990. Benthic foraminiferal assemblages from the eastern Weddell Sea between 68 and 73 S: distribution, ecology and fossilization potential. Marine Micropaleontoly 16, 241-283.

Mannvik, H.P., Wasbotten, I.H., Cochrane, S., 2011. Miljøundersøkelse i Region IX og X Barentshavet 2010, APN-report 5000-03. Akvaplan niva, Tromsø, p. 37.

Mees, J., Boxshall, G.A., Costello, M.J., al, e., 2015. World Register of Marine Species (WoRMS). WoRMS Editorial Board.

Murray, J., 2006. Ecology and applications of benthic foraminifera. Cambridge University Press, New York.

NorwegianPetroleumDirectorate, 2017. Petroleum activity in the Norwegian sector of the Barents Sea – http://www.npd.no/en.

Nyholm, K.G., 1961. Morphogenesis and biology of the foraminifer Cibicides lobatulus. Zoologiska Bidrag Från Uppsala 33, 157-197.

PINRO, 2013. Kola section, in: Karsakov, A. (Ed.).

Polovodova Asteman, I., Hnaslik, D., Nordberg, K., 2015. An almost completed pollution-recovery cycle reflected by sediment geochemistry and benthic foraminiferal assemblages in a Swedish-Norwegian Skagerrak fjord. Marine Pollution Bulletin 95, 126-140.

Polyak, L., Korsun, S., Febo, L.A., Stanovoy, V., Khusid, T., Hald, M., Paulsen, B.E., Lubinski, D.J., 2002. Benthic foraminiferal assemblages from the Southern Kara Sea, a river influenced arctic marine environment. Journal of Foraminiferal Research 32, 252-273.

Polyak, L., Solheim, A., 1994. Late- and postglacial environments in the northern Barents Sea, west of Franz Josef land. Polar Research 13, 197-207.

Qvale, G., 1985. Distribution of foraminifera along the Norwegian Continental Margin, University of Oslo, Oslo, p. 154.

Rayner, N.A., Parker, D.E., Horton, E.B., 2003. Global analyses of sea surface temperature, sea ice, and night marine air temperature since the late nineteenth century. Journal of Geophysical Research 108, 4407-4441.

Rigor, I.G., Colony, R.L., Martin, S., 2000. Variations in surface air temperature observations in the Arctic, 1979–97. Journal of Climate 13, 896-914.

Risebrobakken, B., Moros, M., Ivanova, E.V., Chistyakova, N., Rosenberg, R., 2010. Climate and oceanographic variability in the SW Barents Sea during the Holocene. The Holocene 20, 609-621.

Saher, M., Klitgaard-Kristensen, D., Hald, M., Pavlova, O., Lindal-Jørgensen, L., 2012. Changes in distribution of calcareous benthic foraminifera in the central Barents Sea between the periods 1965–1992 and 2005–2006. Global and Planetary Change 98–99, 81-96.

Sakshaug, E., 1997. Biomass and productivity distributions and their variability in the Barents Sea. ICES Journal of Marine Sciences 54, 341-350.

Sakshaug, E., Slagstad, D., 1992. Sea ice and wind: Effects on primary productivity in the Barents Sea. Atmosphere Ocean 30, 579-591.

Schönfeld, J., Alve, E., Geslin, E., Jorissen, F., Korsun, S., Spezzaferri, S., members.of.the.FOBIMO.workgroup, 2012. The FOBIMO (FOraminiferal BIo-MOnitoring) initiative - towards a standardised protocol for soft-bottom benthic foraminiferal monitoring studies. Marine Micropaleontology, 1-13.

Sejrup, H.P., Birks, H.J.B., Klitgaard Kristensen, D., Madsen, H., 2004. Benthonic foraminiferal distributions and quantitative transfer functions for the northwest European continental margin. Marine Micropaleontology 53, 197-226.

Slubowska, M.A., Koc, N., Rasmussen, T.L., Klitgaard-Kristensen, D., 2005. Changes in the flow of Atlantic water into the Arctic Ocean since the last deglaciation: Evidence from the northern Svalbard continental margin, 80°N. Paleoceanography 20, 1-15.

Smart, C.W., Gooday, A.J., 1997. Recent benthic foraminifera in the abyssal Northeast Atlantic Ocean; relation to phytodetrital inputs. Journal of Foraminiferal Research 27, 85-92.

Smedsrud, L.H., Esau, I., Ingvaldsen, R.B., Eldevik, T., Haugan, P.M., Li, C., Lien, V.S., Olsen, A., Omar, A.M., Otterå, O.H., Risebrobakken, B., Sandø, A.B., Semenov, V.A., Sorokina, S.A., 2013. The role of the Barents Sea in the Arctic climate system. Reviews of Geophysics 51, 415-449.

739 Spielhagen, R.F., Werner, K., Sørensen, S.A., Zamelczyk, K., Kandiano, E.S., Budéus, G., Husum, K., Marchitto,
740 T.M., Hald, M., 2011. Enhanced modern heat transfer to the Arctic by warm Atlantic Water. Science 331, 450-
741 453.

742 Steinsund, P.I., 1994. Benthic foraminifera in surface sediments of the Barents and Kara Seas; Modern and late
743 Quaternary applications. University of Tromsø, Tromsø, p. 111.

744 Sun, X., Corliss, B.H., Brown, C.W., Showers, W.J., 2006. The effect of primary productivity and seasonality on
745 the distribution of deep-sea benthic foraminifera in the North Atlantic. Deep sea research part A: Oceanographic
746 research papers 53, 28-47.

747 Trouet, V., Scourse, J.D., Raible, C.C., 2011. North Atlantic storminess and Atlantic Meridional Overturning
748 Circulation during the last Millennium: reconciling contradictory proxy records of NAO variability. Global and
749 Planetary Change 84-85, 48-55.

750 Veileder02:2013, 2015. Klassifisering av miljøtilstand i vann Økologisk og kjemisk klassifiseringssystem for
751 kystvann, grunnvann, innsjøer og elver, in: Agency, N.E. (Ed.), Trondheim, p. 230.

752 Vinje, T., 2001. Anomalies and Trends of Sea-Ice Extent and Atmospheric Circulation in the Nordic Seas during
753 the Period 1864–1998. Journal of Climate 14, 255-267.

754 Vinje, T., Kvambekk, Å.S., 2001. Barents Sea drift ice characteristics. Polar Research 10, 59-68.

755 Walton, W.R., 1952. Techniques for recognition of living foraminifera. Contribution from the Cushman
756 Foundation of Foraminiferal Research 3, 56–60.

757 Wassmann, P., Carroll, J., Bellerby, R.G.J., 2008. Carbon flux and ecosystem feedback in the northern Barents
758 Sea in an area of climate change: an introduction. Deep Sea Research Part II.

759 Wassmann, P., Duarte, C.M., Augusti, S., Sejr, M.K., 2011. Footprints of climate change in the Arctic marine
760 ecosystem. Global Change Biology 17, 1235-1249.

761 WFD, 2000. Common Implementation Strategy for the Water Framework Directive (2000/60/EC) Guidance
762 Document No. 5. Transitional and Coastal Waters – Typology, Reference Conditions and Classification Systems,
763 Produced by Working Group 2.4 – COAST. Office for official publications of the European communities,
764 Luxemburg, p. 116.

765 Wilson, L.J., Hald, M., Godtliebsen, F., 2011. Foraminiferal faunal evidence of twentieth-century Barents Sea
766 warming. The Holocene 21, 527-537.

767

Figure 1 – Study area
(a) Ocean surface currents of the Norwegian Sea and western Barents Sea. Dashed line indicates an estimation of the present-day position of the Arctic front (after Loeng, 1991). (B) Close up of the western Barents Sea showing core locations along transect in the Bjørnøyrenna trough. Red triangles indicate locations of oil industry exploration wells. Color scale reflects water depth; the contour interval is 50 m. Coordinates of the coring locations are given in Table 1.

Figure 2 – Age model
Upper x-axis: Age models of the cores down to 20 cm, based on the Constant Rate of Supply (CRS) model (Appleby and Oldfield, 1992). Black dots represent dated interval, while open dots with dashed line represent extrapolated ages. Lower x-axis: Excess ^{210}Pb profiles (open dots with error bars). The year 1800 CE, serving as cut off age for samples investigated in the study, is indicated by vertical dashed line.

Figure 3 – Metal concentrations down core
Grain size, TOC and metal concentrations plotted against calendar years (CE): (A) Cumulative sand (black), silt (dark gray) and clay (light gray) content of the cores expressed in volume percentages and total organic carbon (TOC) content (%) (B) Clay content of the cores expressed in volume percentages. To enable comparison between the cores, grey shading (upper x-axis) indicates metal concentrations plotted on the same horizontal scale for each of the cores. (C) Metal concentrations (black plots; lower x-axis) throughout the cores expressed in mg/kg. Note differences in horizontal scale per metal between the cores. To enable comparison between the cores, grey shading (upper x-axis) indicates metal concentrations plotted on the same horizontal scale for each of the cores. Vertical grey lines (plotted on the lower x-axis) indicate boundary between Level I (background) and Level II (no toxic effect; see Supplementary Data A) metal concentrations for the respective metals according to Norwegian sediment quality classification (Bakke et al., 2010).

Figure 4 – Foraminiferal abundance
Range (grey envelope; fossil fauna) in (A) absolute abundance (#/ml) and flux (#/cm^2*yr), (B) number of species and (C) relative abundance (%), for each of the cores. Average core value for the fossil fauna is indicated by thin black line. The value for the live fauna present in the top 5 cm of the sediment is indicated by thick black line.

Figure 5- Density and diversity down core
(A) Foraminiferal flux. (B) Number of species, for calcareous, agglutinated and total fossil fauna (including both calcareous and agglutinated taxa). All data are plotted against calendar years CE based on ages determined by ^{210}Pb dating.

Figure 6 – Foraminiferal abundance down core
Foraminiferal abundances and grain size properties of the sediment cores. (A) Clay (black) and TOC (red) and sand content of the cores; (B) Total calcareous flux (#/cm^2*yr). (C) Relative abundance of most common taxa (black line) and species flux (grey shading). Black dots indicate relative abundance based on > 100 counted specimens; open dots indicate relative abundance based on 60-100 counted specimens; crosses indicate relative abundance based on <60 counted specimens, following Forcino (2012) and Forcino et al., (2015) as elaborated in the text. All data are plotted against calendar years CE based on ages determined by ^{210}Pb dating. (D) Interpreted time intervals as described in Discussion. Color codes illustrate the interpreted environmental conditions reflected by the foraminiferal species (Table 4; see color legend in figure) dominating the representing time interval.

(Fig 1 - double column)

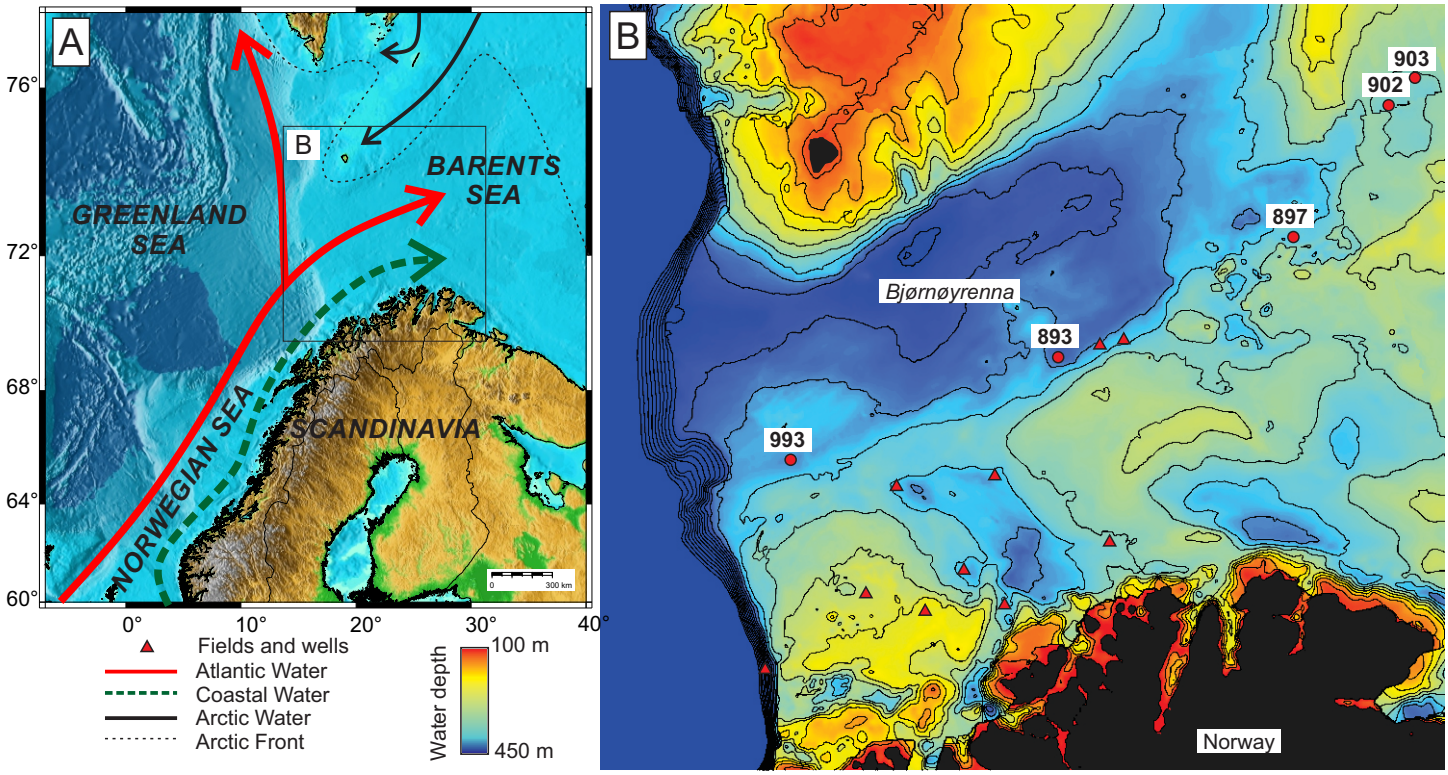

(Fig 2 - 1,5 column)

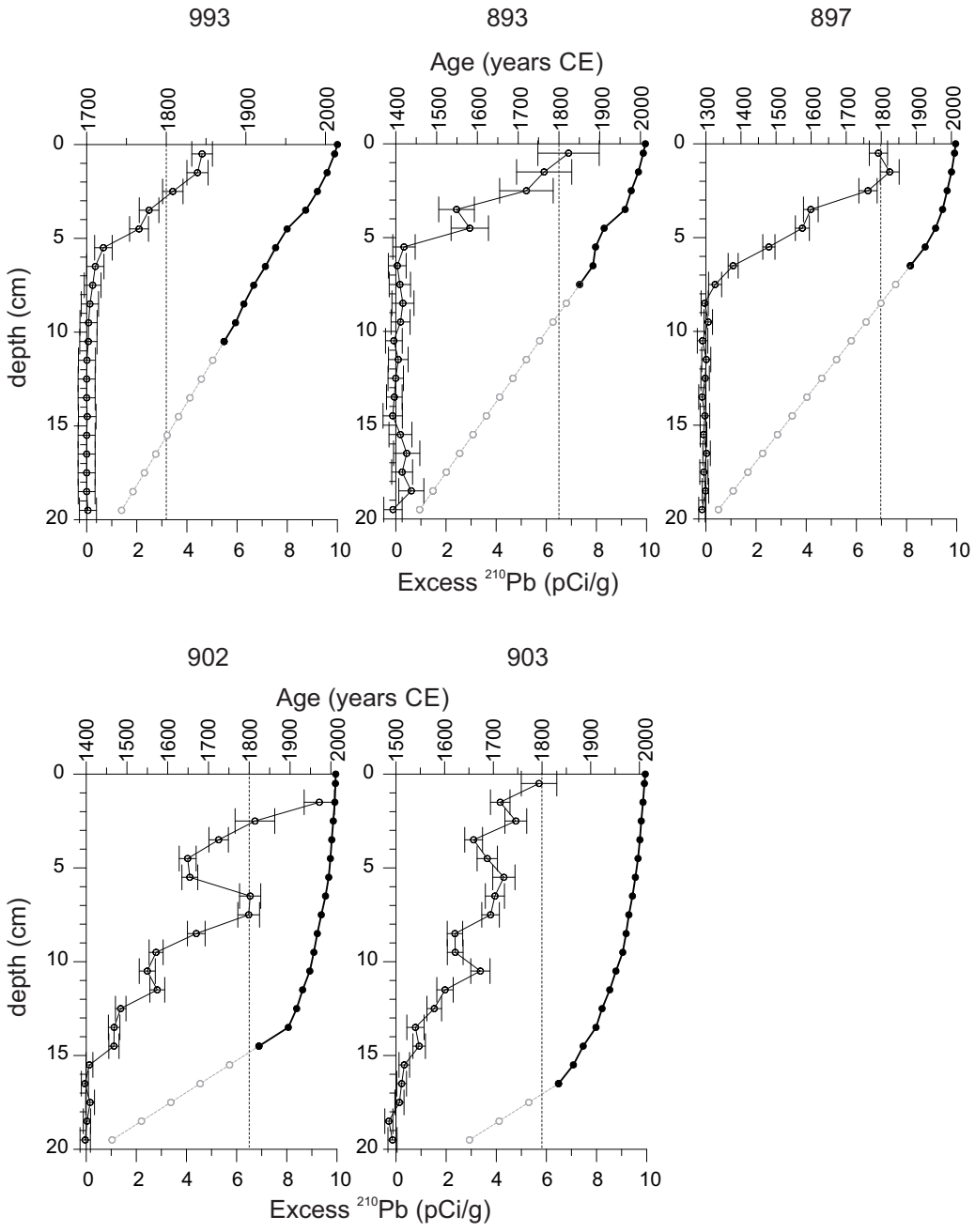

(Fig. 3 - double column)

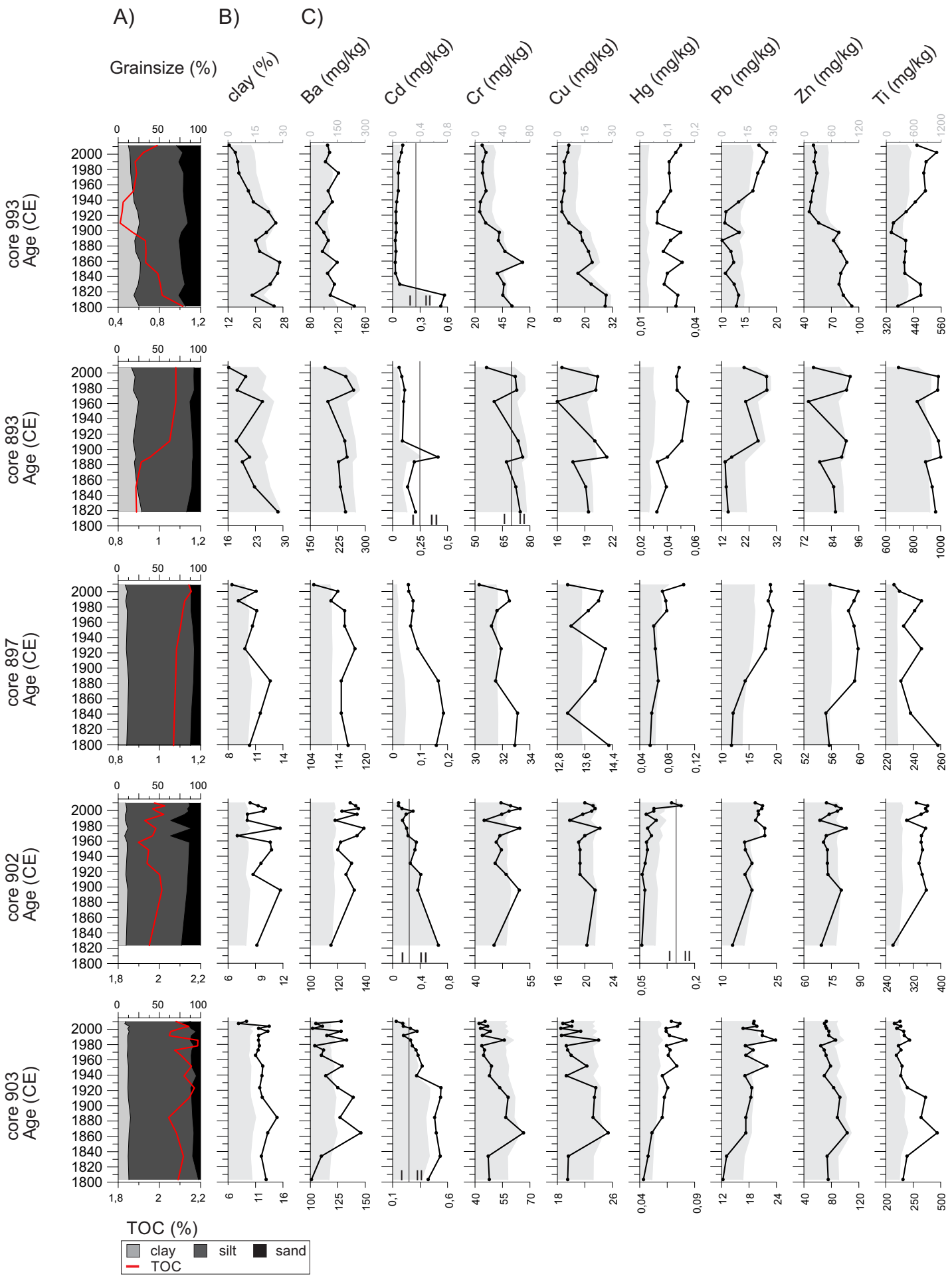

(Fig. 4 - single column)

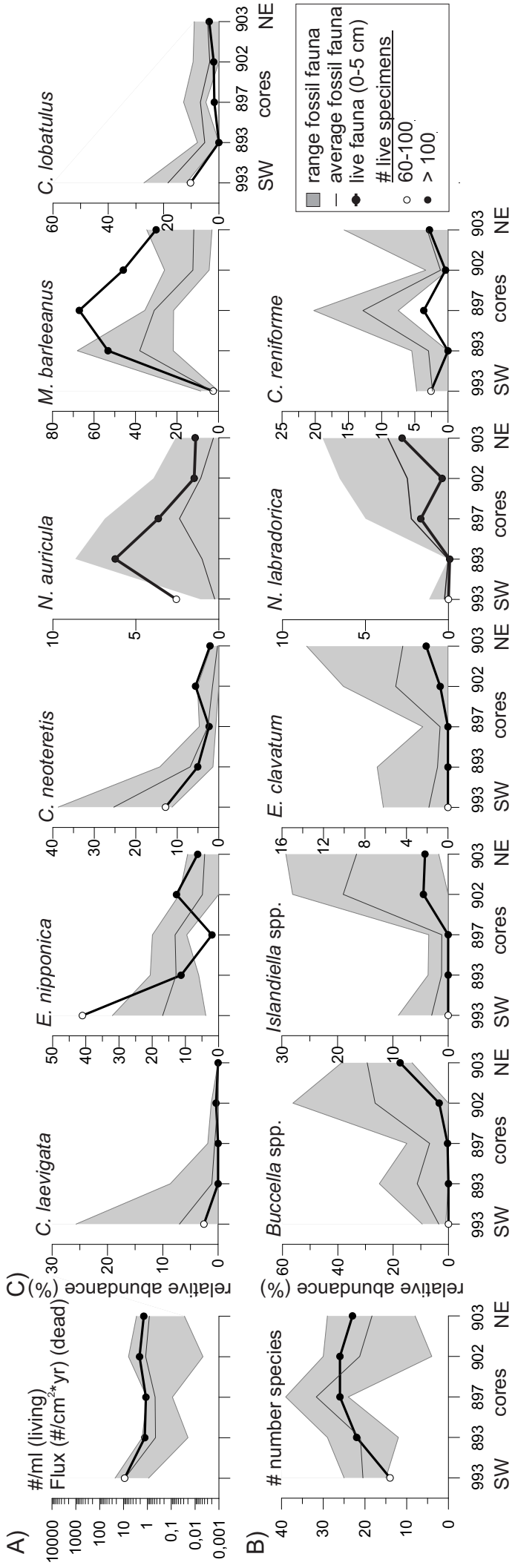

(Fig.5 - 1.5 column)

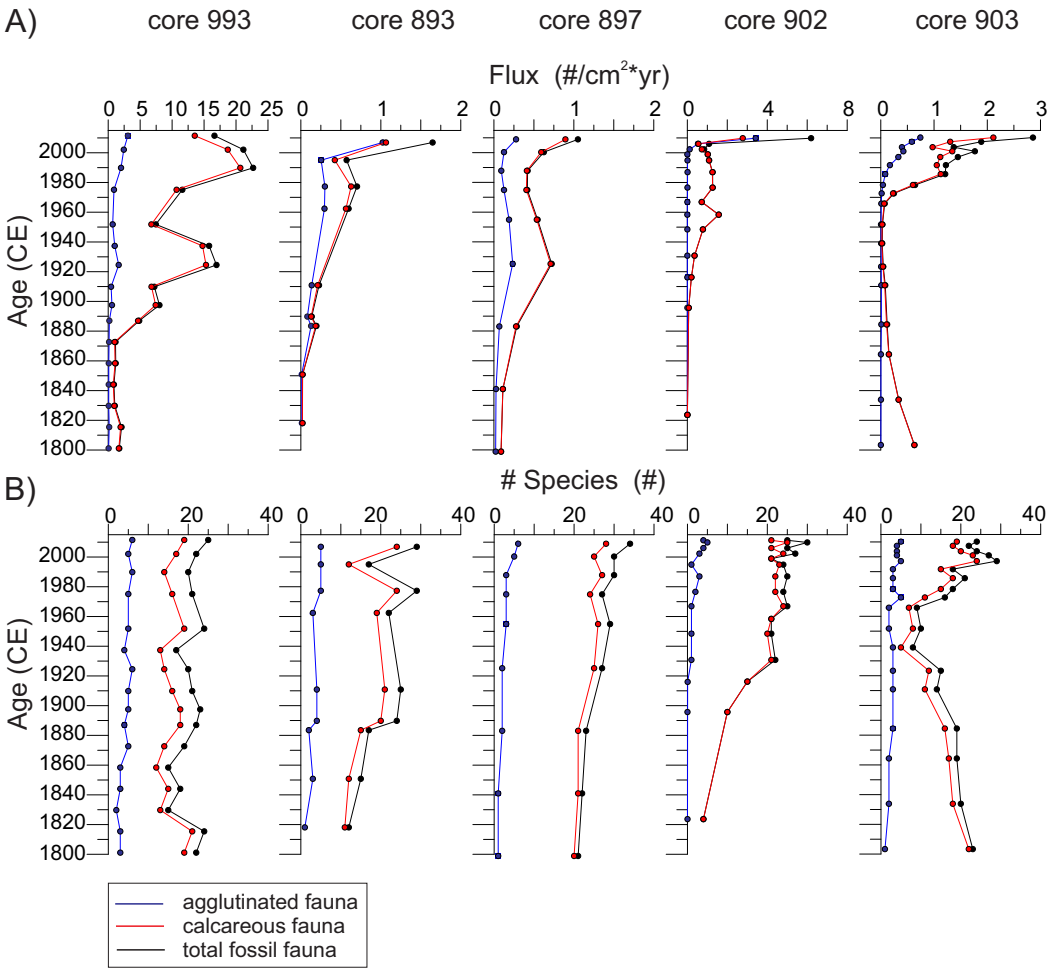

(Fig. 6 - continues on next page- double column)

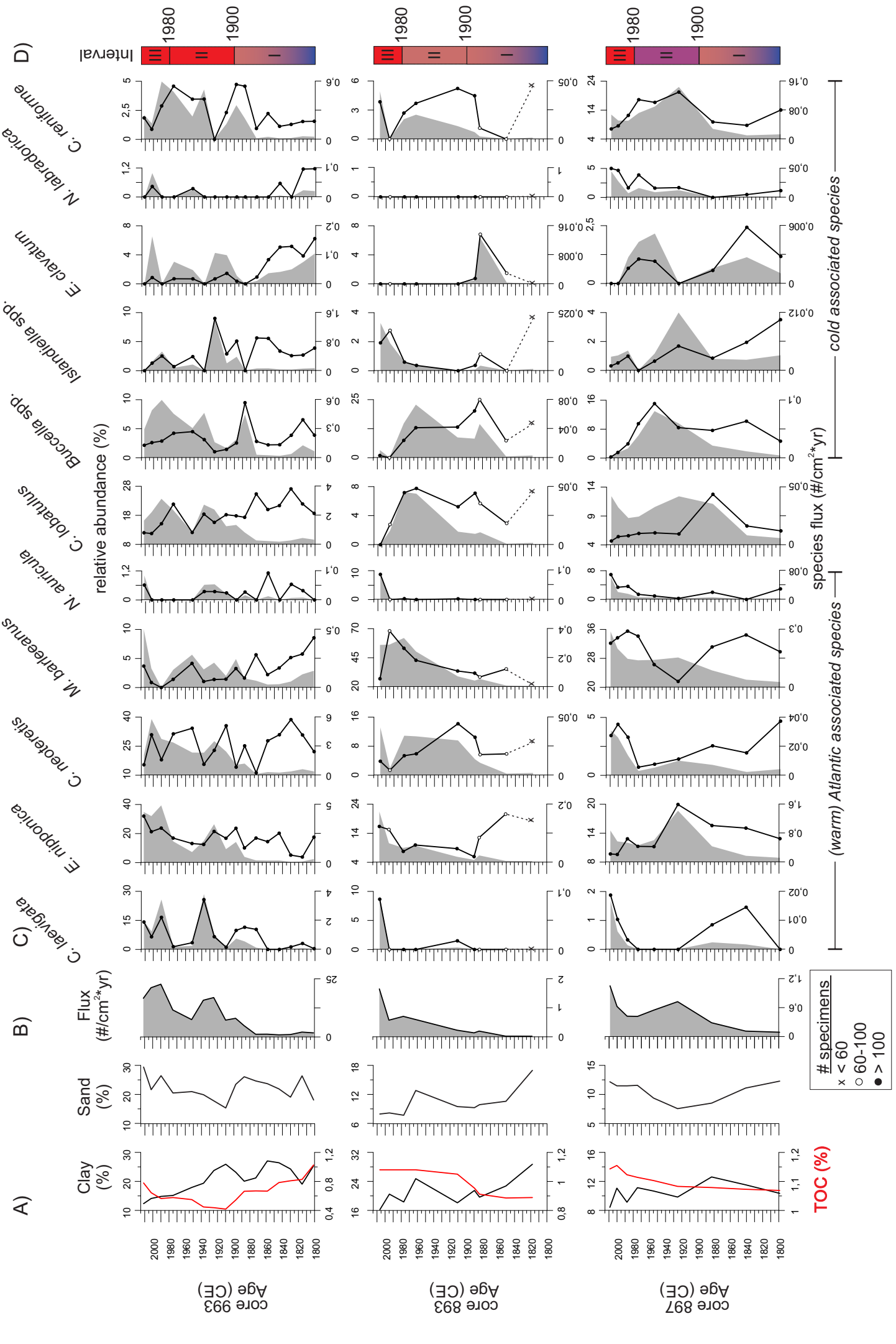

(Fig. 6 - continued from next page- double column)

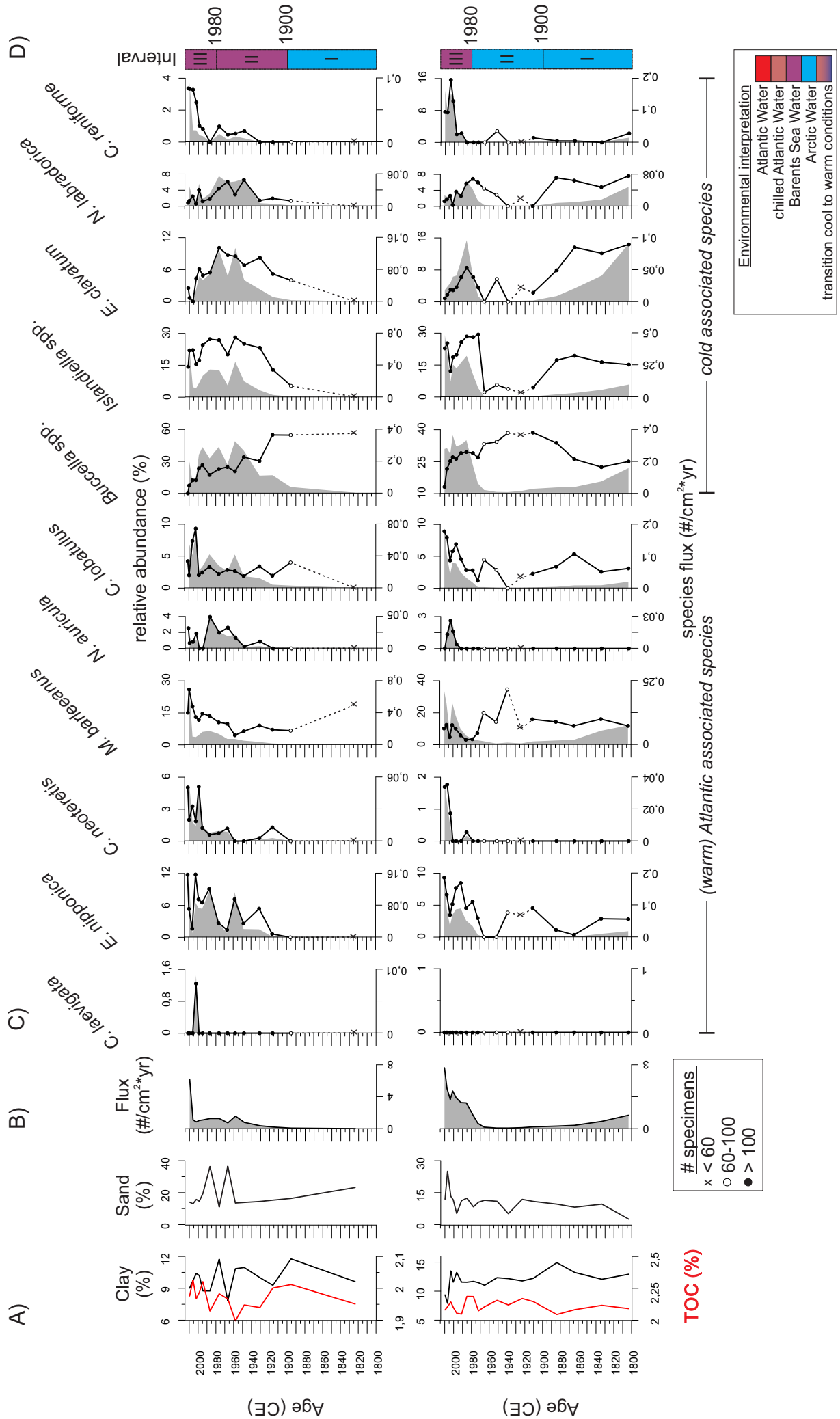

Table 1: Sample material

Geographical location, date of collection and water depth of the analysed sediment cores. Three sediment cores (A, B, C) per station were used in our study, retrieved simultaneously with one multi-corer cast (see description in the text). Below it is clarified which core was used for each of the used methods, i.e. grain size (GS), total organic carbon (TOC), heavy metal concentrations (HM), age model (^{210}Pb) and live and dead foraminiferal assemblage.

	Location	Collected	Water depth	GS	TOC	HM	^{210}Pb	Forams live	Forams dead
993	72°20.144125 N 18°09.412879 E	April 2015	380	C	B	B	B	A	C
893	72°51.441129 N 24°18.658116 E	July 2012	435	B	B	B	C	A	B
897	73°18.983 N 030°15.714 E	July 2012	362	A	A	A	A	B	C
902	73°57.844 N 033°48.926 E	July 2012	333	A	A	A	A	B	C
903	74°04.961 N 034°30.091 E	July 2012	323	A	A	A	A	B	C

Table 2: Age model

Ages (calendar years CE) and sedimentation rates (SR) based on the ^{210}Pb datings. See text for a detailed description of the age model.

	993		893		897	
Core depth	Year (CE)	SR (mm/yr)	Year (CE)	SR (mm/yr)	Year (CE)	SR (mm/yr)
0,5	2011	0,14	2007	0,10	2009	0,16
1,5	2002	0,11	1995	0,08	2000	0,12
2,5	1990	0,08	1977	0,06	1988	0,08
3,5	1975	0,07	1962	0,07	1975	0,08
4,5	1952	0,04	1911	0,02	1955	0,05
5,5	1937	0,07	1890	0,05	1925	0,03
6,5	1925	0,08	1883	0,16	1883	0,02
7,5	1910	0,07	1851	0,03	*(1841)*	
8,5	1898	0,08	*(1818)*		*(1799)*	
9,5	1887	0,10	*(1785)*		*(1757)*	
10,5	1873	0,07	*(1753)*		*(1715)*	
11,5	*(1858)*		*(1720)*		*(1673)*	
12,5	*(1844)*		*(1687)*		*(1630)*	
13,5	*(1830)*		*(1655)*		*(1588)*	*(0,02)*
14,5	*(1815)*		*(1622)*	*(0,03)*	*(1546)*	
15,5	*(1801)*	*(0,07)*	*(1589)*		*(1504)*	
16,5	*(1787)*		*(1557)*		*(1462)*	
17,5	*(1773)*		*(1524)*		*(1420)*	
18,5	*(1758)*		*(1491)*		*(1378)*	
19,5	*(1744)*		*(1459)*		*(1336)*	

	902		903	
Core depth	Year (CE)	SR (mm/yr)	Year (CE)	SR (mm/yr)
0,5	2011	0,69	2010	0,28
1,5	2010	0,69	2007	0,18
2,5	2006	0,26	2004	0,14
3,5	2002	0,27	2001	0,18
4,5	1999	0,30	1997	0,13
5,5	1995	0,25	1992	0,09
6,5	1987	0,13	1986	0,08
7,5	1977	0,10	1978	0,07
8,5	1967	0,10	1973	0,09
9,5	1958	0,12	1966	0,07
10,5	1948	0,10	1952	0,04
11,5	1931	0,06	1939	0,04
12,5	1916	0,07	1923	0,03
13,5	1896	0,05	1911	0,04
14,5	1824	0,01	1884	0,02
15,5	*(1752)*		1864	0,02
16,5	*(1680)*		1834	0,02
17,5	*(1608)*	*(0,01)*	*(1773)*	
18,5	*(1536)*		*(1712)*	*(0,02)*
19,5	*(1463)*		*(1651)*	

Table 3: Sediment properties

Range and average values for TOC, clay, silt and sand content, and heavy metal concentrations.

	TOC (%)	clay (%)	silt (%)	sand (%)	Ba (mg/kg)	Cd (mg/kg)	Cr (mg/kg)	Cu (mg/kg)	Hg (mg/kg)	Pb (mg/kg)	Zn (mg/kg)	Ti (mg/kg)
993	0,4-1	12-27	49-64	15-29	89-144	0,03-0,6	24-63	10-29	0,02-0,03	10-18	46-92	342-540
average	0,7	21	57	22	109	0,1	37	17	0,03	13	66	433
893	0,9-1,1	16-25	54-76	8-17	190-268	0,06-0,4	56-76	16-21	0,03-0,06	13-28	74-92	657-1000
average	1,0	21	69	10	234	0,2	69	19	0,04	20	85	918
897	1,1-1,2	8-13	77-83	8-12	105-117	0,06-0,2	30-33	13-14	0,06-0,10	12-19	55-60	200-461
average	1,1	11	79	11	113	0,1	32	14	0,07	17	58	239
902	1,9-2,0	8-12	55-77	11-37	115-139	0,08-0,7	43-53	18-22	0,06-0,16	13-22	69-83	261-362
average	2,0	10	72	18	128	0,3	48	20	0,08	19	75	339
903	2,0-2,2	8-15	67-85	3-25	101-146	0,1-0,5	42-66	18-25	0,04-0,08	12-24	65-103	247-632
average	2,1	12	78	11	119	0,3	49	21	0,06	18	78	311

Table 4 Foraminifera
Summary of the most common benthic foraminifera species with associated water mass and environmental interpretation

		Fauna	Environmental preferences	Reference
Atlantic water	warm associated species	*C. laevigata*	warm, saline	(e.g. Altenbach et al., 1999; Hald and Steinsund, 1992; Jennings et al., 2004; Mackensen and Hald, 1988; Qvale, 1985; Saher et al., 2012; Sejrup et al., 2004; Steinsund, 1994)
		E. nipponica	warm	
		C. neoteretis	chilled Atlantic	(e.g. Gooday and Lambshead, 1989; Jennings et al., 2004; Mackensen and Hald, 1988)
		M. barleeanus	degraded organic matter fine grained sediments	(e.g. Dijkstra et al., 2013; Linke and Lutze, 1993; Mackensen et al., 1985)
		N. auricula	warm degraded organic matter	(e.g. Dijkstra et al., 2013; Korsun and Hald, 1998)
		C. lobatulus	epifaunal in sandy sediments high energy environment	(e.g. Hald and Steinsund, 1996; Mackensen et al., 1985; Nyholm, 1961; Steinsund, 1994)
Arctic water	cold associated species	*Buccella* spp.	cool, seasonal sea ice pulsed phytodetritus	(e.g. Hald and Korsun, 1997; Hald and Steinsund, 1992; Korsun and Hald, 2000; Polyak et al., 2002; Polyak and Solheim, 1994; Sejrup et al., 2004; Wilson et al., 2011)
		E. clavatum	low salinity and temperature	
		Islandiella spp.	cool	
		N. labradorica	cool, Arctic Front pulsed phytodetritus	
		C. reniforme	cooled saline water	(e.g. Bartels et al., 2017; Mackensen et al., 1985; Sejrup et al., 2004; Slubowska et al., 2005)